Liu *et al. Satellite Navigation* (2022) 3:1
https://doi.org/10.1186/s43020-022-00063-5

Satellite Navigation
https://satellite-navigation.springeropen.com/

ORIGINAL ARTICLE

Open Access

Multiplexing modulation design optimization and quality evaluation of BDS-3 PPP service signal

Cheng Liu[1], Zheng Yao[2*], Dun Wang[3], Weiguang Gao[1], Tianxiong Liu[4], Yongnan Rao[5], Dongjun Li[3] and Chengeng Su[1]

Abstract

The Precise Point Positioning (PPP) service of BeiDou-3 Navigation Satellite System (BDS-3) is implemented on its Geostationary Earth Orbit (GEO) satellites. However, its signal design is limited by the actual power of satellite and other conditions. Furthermore, the design needs to fully consider the compatibility of different service phases. Starting from the actual state of the BDS-3 GEO satellite, this paper studies the multiplexing modulation of the BDS PPP service signal that is based on the Asymmetric Constant Envelope Binary Offset Carrier (ACE-BOC) technique and proposes several feasible schemes for this signal. Comparison and optimization of these techniques are made from the aspects of transmission efficiency, multiplexing efficiency, and service forward compatibility. Based on the Type-III ACE-BOC multiplexing modulation technique, phase rotation and intermodulation reconstruction techniques are proposed to suppress the intermodulation interference issue. Finally, a signal based on improved ACE-BOC multiplexing is designed. The quality of the proposed signal was continuously monitored and tested using large-diameter antennas. The evaluation results show that the power spectrum deviation of the signal is 0.228 dB, the correlation loss is 0.110 dB, the S-curve slope deviation is 1.558% on average, the average length difference between the positive/negative chip and the ideal chip is only 0.0006 ns, and the coherence between the carrier and the pseudo code is 0.082°. All quality indicators are satisfactory, indicating that the proposed signal multiplexing modulation technique is an ideal solution that meets all the requirements of the design constraints, and can achieve efficient information broadcasting and forward compatibility of the BDS PPP service.

Keywords: BeiDou, Precise point positioning, Constant envelope multiplexing, ACE-BOC, Inter-modulation construction

Introduction

Precise Point Positioning (PPP) has the characteristics of wide service coverage, uniform accuracy distribution, and a small number of ground reference stations needed (Héroux & Kouba, 2001; Jin & Su, 2020). It is an important technique for wide-area high-precision navigation and positioning (Hein, 2020). The PPP system was initially requested by enterprises to be implemented using a custom data format and broadcast via the International Maritime Communication Satellite (InMarSat) thus providing paid commercial services. Representative PPP services include Navcom's StarFire, Trimble's OmniSTAR and RTX, Fugro's StarFix/SeaStar, Oceaneering International's C-Nav, Hexagon's VeriPos and TerraStar, etc.

In recent years, with the technological development and capability enhancement of various satellite navigation systems, the trend is to provide embedded open or free PPP services directly from basic satellite constellations

*Correspondence: yaozheng@tsinghua.edu.cn
[2] Department of Electronic Engineering, Tsinghua University, Beijing 100084, China
Full list of author information is available at the end of the article

(Guo et al., 2019). The European Galileo navigation satellite system (Galileo) is designed to provide high-precision free PPP services with global coverage and with an expected accuracy of 0.2 m and a data rate of 500 bit/s on its E6-B signal (Hayes, 2018; Hayes & Hahn, 2019). Japan's Quasi-Zenith Satellite System (QZSS) uses its L6D signal to provide a Centimeter Level Augmentation Service (CLAS) based on PPP-RTK (Real-Time Kinematic) technology. According to the QZSS Performance Standard (PS) and its Interface Control Document (ICD) (IS-QZSS-L6-001) released in November 2018, CLAS service broadcasts a data rate of up to 2000 bit/s and can reach centimeter-level accuracy within 1 min (Cabinet Office, 2018a, b). In addition, QZSS is also using its L6E signal on Block II satellites to carry out the technical verification of the wide-area centimeter-level enhanced services covering the Asia–Pacific region (Li, 2017; QZSS, 2018). The Russian GLONASS also announced its PPP service plan with an expected accuracy of 0.1 m, which will be mainly used in precision engineering, Emergency Road Service (ERS), and unmanned driving (Revnivykh, 2019).

The BeiDou-3 Navigation Satellite System (BDS-3) also attaches a great importance to the design and development of PPP services (Yang et al., 2019). On December 27, 2019, at the press conference for the first anniversary of the BDS-3, it was announced that BDS-3 would provide PPP service. Additionally, the BeiDou Navigation Satellite System (BDS) Application Service System (Version 1.0), BeiDou System Space Signal Interface Control File PPP-B2b (Beta Version), and other related documents were officially released (China Satellite Navigation Office, 2019a, c, d). The BDS PPP service is realized through the broadcasting of the B2b signal from BDS Geostationary Earth Orbit (GEO) satellites (called PPP-B2b signal). The implementation of this service is carried out in two phases. Starting in 2020, BDS-3 uses the PPP-B2b signal in-phase component from the first three GEO satellites to provide open high-precision positioning services with a data rate of 500 bit/s for the users in China and surrounding areas. After that, BDS will use the follow-on GEO satellites to increase the broadcast rate, expand the service range, and further improve the positioning accuracy and reduce the convergence time.

PPP service is an important measure for BDS to improve its competitiveness in high-precision applications. However, the design of the BDS PPP service signal is subject to many restrictions, which brings challenges to this work. First, the B2a band on BDS-3 GEO satellites is for Satellite-Based Augmentation Service (SBAS), and must strictly abide by the standards and requirements of the International Civil Aviation Organization (ICAO). Thus, the realization of the PPP-B2b signal cannot affect the status of the B2a signal. Secondly, although the PPP-B2b signal is mainly used for data transmission rather than ranging, it still requires a sufficiently high signal quality to ensure the reliable and stable transmission of PPP corrections. Finally, due to the possibility of service upgrades in the future, the PPP-B2b signal design needs to consider the issue of future compatibility.

Starting from the current actual state of the BDS-3 GEO satellite, this paper explores PPP service signals based on the Asymmetric Constant Envelope Binary Offset Carrier (ACE-BOC) multiplexing technique (Yao et al., 2016). Several feasible multiplexing modulation techniques are proposed. The comparison and optimization of the techniques are made from the aspects of transmission efficiency, multiplexing efficiency, and service forward compatibility. Compared with other techniques, an improved Type-III ACE-BOC is more suitable for the realization of PPP services. Thus, this technique is adopted on the first three GEO satellites. A large-aperture antenna is further used for continuous monitoring and quality testing of the broadcast signal. According to the evaluation, the average power spectrum deviation of PPP-B2b is only 0.228 dB, the correlation loss is 0.110 dB, the maximum deviation is 0.092 ns, the S-curve slope deviation is 1.558%, and the averaged length difference between the positive/negative chip and the ideal chip is 0.0006 ns, and the coherence between the carrier and the pseudo code is 0.082°. The results show that the proposed signal meets the design requirements for all parameters. It has good radio frequency characteristics and can achieve efficient information broadcast and service compatibility. Therefore it is an ideal BDS-3 PPP service signal solution.

Multiplexing requirements of GEO B2 signal

The B2 band of a BDS-3 GEO satellite contains two signals, B2a and B2b. Among them, B2a signal is for Dual-Frequency Multi-Constellation (DFMC) SBAS service, referred to as the BDSBAS-B2a signal (SBAS IWG, 2016a, b). According to the requirements of the DFMC SBAS standard from the SBAS Interoperability Working Group (SBAS IWG) and the ICAO, BDSBAS-B2a must adopt the same spreading modulation of GPS/ Wide Area Augmentation System (WAAS) L5 signals, which is QPSK with the chip rate of 10.23 megachips per second (Mcps). Furthermore, the received minimum radio frequency (RF) signal strength must be greater than − 158.5 decibel watt (dBW) (China Satellite Navigation Office, 2019b; ICAO, 2018). According to the actual power capability of satellites, in order to ensure that the received signal strength of B2a meets the requirements of the ICAO standard, for GEO satellites, the power ratio of the B2a signal to the B2b signal should be 2:1.

The design of the PPP-B2b signal is carried out with the above constraints. Since BDS-3 has three different types of satellites in three different types of orbits, some B2 signal components may be used to support different services. The use of separate transmission links for B2b and B2a signals can ensure that the power and phase adjustments of the two sub-bands are independent, but the interval between the power spectral main lobes of the signals located on two sub-bands of B2 is only 10.23 MHz. Separate transmissions induce a higher complexity in the filter design. More importantly, combining signals on these two sub-bands into a constant envelope signal can not only save the number of the High-Power Amplifier (HPA), thereby saving the cost, volume, and power consumption of the load, but also ensure a high correlation of link. Therefore, multiplexing the PPP-B2b component with other signal components on the B2 band into a constant envelope composite signal and sharing the transmit aperture becomes a necessary design constraint.

Most of the typical Constant Envelope Multiplexing (CEM) techniques are proposed to meet the combined emission requirements of signal components at the same central frequency (Butman & Timor, 1972; Dafesh & Cahn, 2001; Spilker & Orr, 1998). The design requirements of Galileo and BDS-3 have given birth to the emergence of a dual-frequency constant envelope multiplexing technology (Dafesh & Cahn, 2011; Guo et al., 2016; Huang et al., 2015; Lestarquit et al., 2008; Yao et al., 2016; Zhang et al., 2013). The first dual-frequency CEM technique is the Alternative Binary Offset Carrier (AltBOC) technique which is used in the Galileo E5 band (Lestarquit et al., 2008). However, the number, power relationship, and phase relationship of signal components involved in AltBOC are strictly fixed. It is desirable to have a unified multiplexing technique with a flexible power configuration when multiplexing the B2 components on different types of satellites. Therefore, it is necessary to use a dual-frequency multiplexing technique that is more flexible than AltBOC.

The advantages of the ACE-BOC multiplexing method (Yao et al., 2016) in dual-frequency multi-component multiplexing and flexible power distribution make it possible to flexibly design and implement a variety of B2 signal solutions. The general form of an ACE-BOC multiplexed signal can be expressed as ACE-BOC $(m, n, \boldsymbol{p})$, where m represents the sub-carrier frequency normalized with 1.023 MHz, n represents the spreading code rate normalized with 1.023 MHz, $\boldsymbol{p} = \left(P_{\mathrm{UI}}, P_{\mathrm{LI}}, P_{\mathrm{UQ}}, P_{\mathrm{LQ}}\right)$ represents the power ratio between the components in the composite ACE-BOC signal, UI, LI, UQ, and LQ correspond to the upper sideband I branch, the lower sideband I branch, the upper sideband Q branch, and the lower sideband Q branch, respectively.

The ACE-BOC multiplexing technique is very flexible in selecting the number of components and the power ratio of each component. The elements of the vector $\boldsymbol{p}$ can be any non-negative real number. If the value of a certain element is zero, it means that the corresponding component is not broadcast. This feature allows system designers to flexibly optimize the number of transmitted signal components according to the characteristics of the service and to allocate signal power accordingly. In the final B2 signal ACE-BOC technique of Medium Earth Orbit (MEO) or Inclined Geo-Synchronous Orbit (IGSO) satellites and GEO satellites, the number of components and the power ratio of each component are different.

Constrained by the International Telecommunication Union (ITU) on the spectrum envelope, the code rate of each component of the composite B2 signal is $f_{\mathrm{c}} = 10.23$ MHz, corresponding to $n = 10$. Since the central frequencies of the B2a and B2b bands are $f_{\mathrm{L}} = 1176.45$ MHz and $f_{\mathrm{U}} = 1207.14$ MHz, respectively, the subcarrier frequency of ACEBOC signal is $f_{\mathrm{s}} = \left(f_{\mathrm{U}} - f_{\mathrm{L}}\right)/2 = 15.345$ MHz, corresponding to $m = 15$. The optimization of the vector $\boldsymbol{p}$ needs to take into account multiple constraints, such as the data broadcast rate, the on-board multiplexing efficiency, and the forward and backward compatibility of the service, which will be analyzed in detail in the next section.

PPP-B2b schemes based on ACE-BOC multiplexing

QPSK signal based on type-II ACEBOC

For the PPP-B2b signal with a total message rate of 500 bit/s, a potential modulation technique is to use two components in I-Q quadrature structure with equal power, which is the same as BDSBAS-B2a. In this technique, the message rate of both branches is 250 bit/s. Since in GEO satellites, B2a signal and B2b signal should be allocated power at a ratio of 2:1, the composite B2 signal corresponds specifically to the Type-II ACE-BOC signal (Yao et al., 2016), with $\boldsymbol{p} = (1, 2, 1, 2)$.

This technique can guarantee that the total Power Spectral Density (PSD) of B2 signal in BDS GEO satellites is similar to that of the B2 signals in MEO and IGSO satellites and can obtain the maximum multiplexing efficiency among all solutions, which means that each signal component can obtain the maximum actual power. The actual power proportion and the multiplexing efficiency of each component are shown in Table 1. The corresponding constellation diagram and the PSD under the infinite bandwidth are shown in Figs. 1 and 2, respectively.

The main advantage of using Type II ACE-BOC is that it can achieve the maximum multiplexing efficiency. However, it is not optimal for PPP services. The main problems are twofold.

Table 1 Power proportion and multiplexing efficiency

B2a-I: B2a-Q: B2b-I: B2b-Q	Power proportion of different signals				Multiplexing efficiency	Phase relationship between B2b-I and B2a-I
	B2a-I	B2a-Q	B2b-I	B2b-Q		
2:2:1:1	0.2737	0.2737	0.1369	0.1369	82.11%	0°

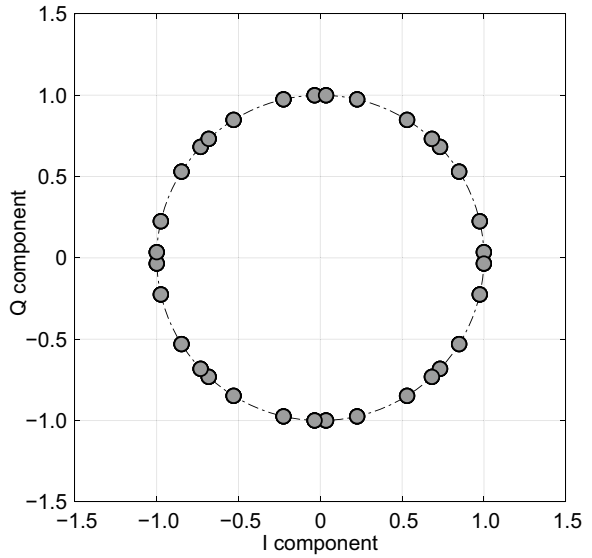

Fig. 1 Multiplexing modulation constellation of Type-II ACE-BOC

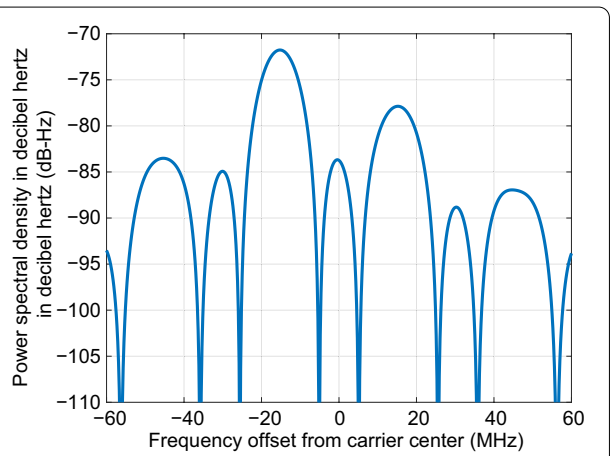

Fig. 2 Multiplexing modulation power spectral density of Type-II ACE-BOC

First, adopting Type II ACE-BOC means that the PPP-B2b signal must be divided into I and Q branches, with 2 synchronous headers and 2 Cyclic Redundancy Check (CRC) placeholders, thereby wasting the precious byte resources of PPP-B2b as the data broadcast channel. For receiving, Type II ACE-BOC also needs to receive the I and Q branch signals separately, demodulate the message information of the two branches, and then combine them together, which increases the complexity of the receiving processing.

Secondly, in the second phase of BDS development, the PPP-B2b broadcast rate is planned to be increased. In terms of design, the two-phase service implementation should have compatibility and continuity to ensure the smooth transition and compatible use for users. Therefore, if the PPP-B2b signal in the first phase adopts the I-Q quadrature modulation, then as the subsequent broadcast rate increases, it will be necessary to change the data rate, signal modulation mode, and corresponding coding mode of both the I and Q branches, forcing the receiver to make corresponding modifications, which is not conducive to user equipment compatibility.

BPSK signal based on Type-III ACEBOC

Another potential PPP-B2b signal solution is to use a single Binary Phase-Shift Keying (BPSK) component. The main difference between this technique and the Type-II ACE-BOC technique is that the I-Q quadrature components with 250 bit/s data rate each are combined into a single branch with the data rate of 500 bit/s, and the composite B2 signal corresponds to a Type-III ACEBOC signal (Yao et al., 2016) with $\boldsymbol{p} = (1, 1, 0, 1)$. The corresponding constellation diagram and the PSD under the infinite bandwidth are shown in Figs. 3 and 4, respectively.

The main advantage of using the Type III ACE-BOC technique is that it can achieve a smooth transition and compatible upgrade for users in the two service phases before and after upgrading and make the design architecture of the entire PPP-B2b service signal more regular and clearer.

Specifically, as shown in Table 2, because the Q branch is reserved, the PPP service in the first phase can be provided through the broadcast of the PPP-B2b I branch of the first three GEO satellites. The requirements for adding data message content and increasing data rate can be achieved by the PPP-B2b Q branch of subsequent backup GEO satellites, while keeping the original I branch signal unchanged. In this way, the I branch signals of each GEO satellite in different service phases are the same for all

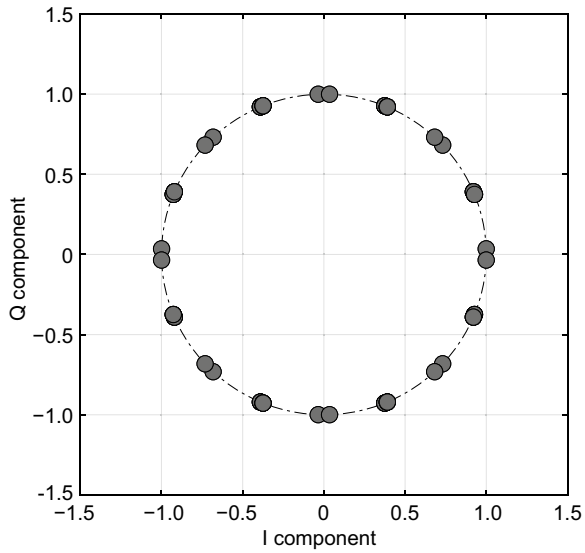

Fig. 3 Multiplexing modulation constellation of Type-III ACE-BOC

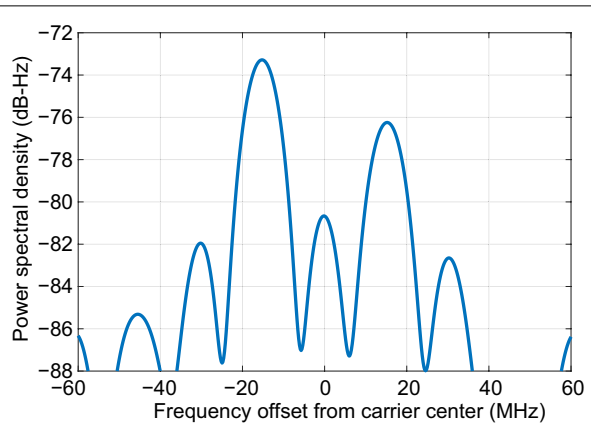

Fig. 4 Multiplexing modulation power spectral density of Type-III ACE-BOC

users, thereby ensuring service compatibility and continuity, as shown in Fig. 5.

Secondly, this technique can save a set of synchronization headers and CRC placeholders. The general synchronization header length of the BDS open service signal message frame structure is 8 bit, the CRC length is 24 bit, and the total length of a set of synchronization header + CRC is 32 bit. According to the customized compressed message format of the BDS PPP service, the bits saved can be used to broadcast the orbit correction of 1 satellite, the clock correction of 2 satellites, or the mask number of 32 satellites, thereby improving the broadcast efficiency.

Finally, the use of Type III ACE-BOC multiplexing also enables the PPP-B2b I branch to use ranging codes with the same characteristics as the B2b open service signal I branch broadcast on MEO and IGSO satellites, as well as the same LDPC coding techniques and parameters (Huang et al., 2017, 2019), which is more convenient for receiver design.

However, the direct use of Type III ACE-BOC technique also brings some drawbacks, mainly the influence of the intermodulation component. Table 3 shows the actual power proportion and multiplexing efficiency of each component with the Type III ACE-BOC technique (Liu et al., 2020). It can be seen that, on the one hand, when the phase relationship between the PPP-B2b I branch and the BDSBAS-B2a I branch is 0°, the intermodulation term introduced to maintain the constant envelope of the composite signal accounts for a relatively large proportion of power, resulting in a decrease in multiplexing efficiency. On the other hand, the intermodulation component will interfere with the useful components, which causes not only a certain deviation between the actual power relationship and the design input, but also the non-orthogonally between a part of the intermodulation component and the useful component, resulting in the distortion of the signal correlation function and an increase in the code phase deviation between components.

GEO B2 composite signal based on optimized ACE-BOC

From the comprehensive comparison and analysis, it can be seen that the QPSK technique of PPP-B2b signals based on Type II ACE-BOC is unfavourable for the overall BDS PPP service; while the BPSK technique of PPP-B2b signals based on Type III ACE-BOC multiplexing is conducive to the realization of services in terms of transmission efficiency, compatibility, and receiver design. However, it has the drawback of being affected by

Table 2 Overall plan of PPP-B2b

Signal	Components name	Carrier frequency (MHz)	Modulation type	Data rate in sps (symbol per second)	First 3 GEO satellites	Subsequent GEO satellite
PPP-B2b	I	1207.14	BPSK(10)	1000	Available	Available
	Q	1207.14	TBD	TBD	NA	Available

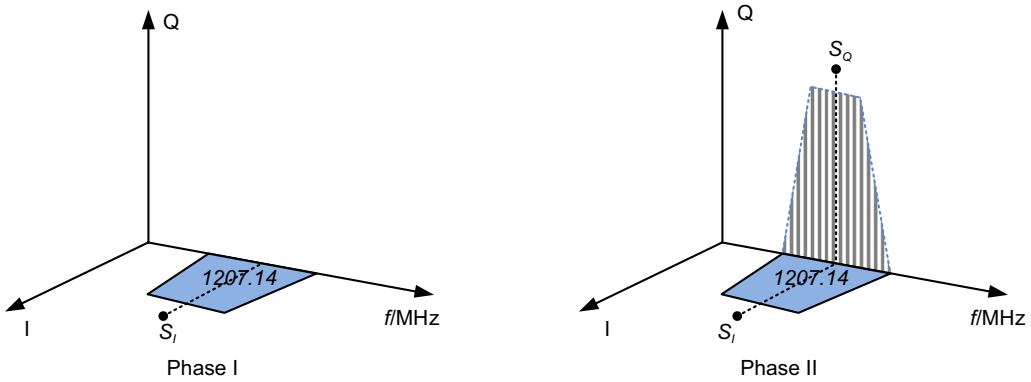

Fig. 5 Evolution of PPP-B2b signal

Table 3 Actual power and multiplexing efficiency of each component of Type-III ACE-BOC when the phase relationship between I-components is 0

B2a-I: B2a-Q: B2b-I: B2b-Q	Power proportion of different signals				Multiplexing efficiency	Phase relationship between B2b-I and B2a-I
	B2a-I	B2a-Q	B2b-I	B2b-Q		
1:1:1:0	0.2374	0.2026	0.2026	0	64.27%	0

the intermodulation component. If based on the Type III ACE-BOC technique, the influence of intermodulation components can be suppressed, and the multiplexing efficiency can be improved, thus it is an ideal technique for BDS-3 PPP services.

Phase rotation

A phase rotation process is proposed for the PPP-B2b I branch component focusing on the problem that the intermodulation term introduced to maintain a constant envelope of the composite B2 signal accounts for a relatively large proportion of power. By changing the signal component phase look-up table, the phase relationship between the PPP-B2b I branch and the BDSBAS-B2a signal I and Q branch is changed from 0° to 45°, as shown in Fig. 6. Since the phase rotation changes only the relative phase relationship between the two signals of BDSBAS-B2a and PPP-B2b, rather than the phase relationship between different components of the same signal, there is no impact on the receiver that receives and uses the PPP-B2b signal alone.

Table 4 shows the actual power and multiplexing efficiency of each component under Type III ACE-BOC multiplexing when the phase relationship between the I branches of B2a and B2b is 45°. Comparing Tables 3 and 4, it can be seen that the proportion of intermodulation terms is reduced through the phase rotation processing, and the multiplexing efficiency is significantly improved, achieving the same efficiency as the QPSK technique based on Type II ACE-BOC. This identity is no coincidence. Comparing Table 4 and Table 2, it is not difficult to see that the phase rotation processing can be approximated as letting the B2b-I and B2b-Q components of Type II ACE-BOC multiplexing technique use the same spreading sequence and data message, so that the signs of these two components are identical at any time, thus forming a BPSK component whose phase relationship with the B2a I branch is 45°.

However, if the same spreading sequence is used, the assumption that the components are completely orthogonal with each other will no longer be true. The remaining intermodulation term will still interfere with the useful components, thus further optimization needs to be carried out on the basis of phase rotation.

Intermodulation component suppression

Using CEMIC technology (Yao & Lu, 2017; Yao et al., 2017), the frequency domain distribution of the intermodulation component in constant envelope multiplexing can be adjusted, and the Type-III ACE-BOC with the 45° phase rotation is further optimized. In the iterative optimization process, the suppression of the intermodulation component can be achieved by setting the weight for the coefficient of the intermodulation term that causes obvious interference to the useful signal to zero.

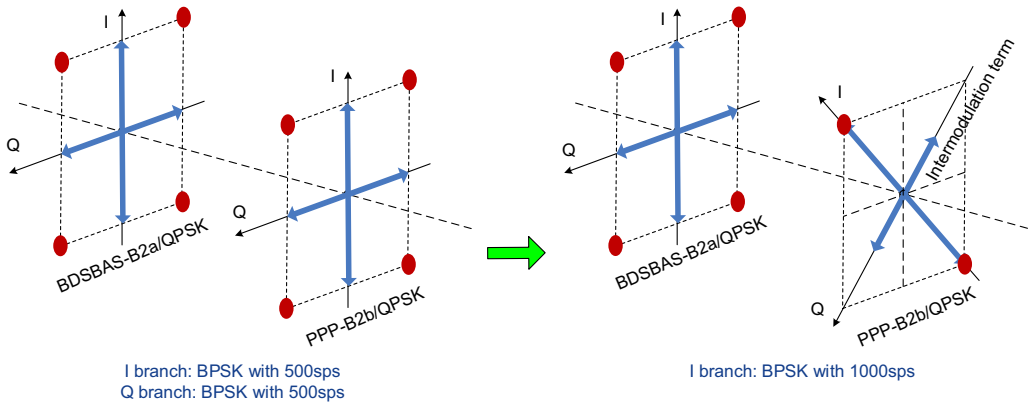

Fig. 6 Phase rotation of PPP-B2b_I

Table 4 Actual power and multiplexing efficiency of each component of Type-III ACE-BOC when the phase relationship between I-components is 45°

B2a-I: B2a-Q: B2b-I: B2b-Q	Power proportion of different signals				Multiplexing efficiency	Phase relationship between B2b-I and B2a-I
	B2a-I	B2a-Q	B2b-I	B2b-Q		
1:1:1:0	0.2737	0.2737	0.2737	0	82.11%	45°

The detailed theoretical derivation of this suppression process can be found in (Yao et al., 2017). To illustrate the principle of this process, let us consider a general multi-carrier multiplexing of N BPSK signal component in which the baseband composite signal of the useful component can be expressed as

$$s_d(t) = \sum_{i=1}^{N} \sqrt{P_i} \exp\left(j\varphi_i\right) s_i(t) sc_i(t) \tag{1}$$

where $s_i(t)$ represents the ith baseband signal, P_i, φ_i and $sc_i(t)$ are its corresponding power, phase, and subcarrier waveform, respectively. We take all possible values of $\left[\, s_1(t)\ s_2(t)\ \cdots\ s_N(t) \,\right]$ as the rows of the matrix $\boldsymbol{S}$ with $2^N \times N$ dimensions, and denote the ith column of $\boldsymbol{S}$ as s_i, which is the vector form of $s_i(t)$. We take all L possible values of $\left[\, sc_1(t)\ sc_2(t)\ \cdots\ sc_N(t) \,\right]$ as the rows of the matrix $\boldsymbol{E}$ with $L \times N$ dimensions, and denote the ith column of $\boldsymbol{E}$ as $\boldsymbol{\kappa}_i$, which is the vector form of $sc_i(t)$. Thus, the vector form of $s_d(t)$ can be expressed as $\tilde{\boldsymbol{S}}\boldsymbol{c}_s$, where

$$\boldsymbol{c}_s = \left[\, \sqrt{P_1}\exp(j\varphi_1)\ \sqrt{P_2}\exp(j\varphi_2)\ \cdots\ \sqrt{P_N}\exp(j\varphi_N) \,\right]^{\mathrm{T}} \tag{2}$$

and

$$\tilde{\boldsymbol{S}} = \left[\, \boldsymbol{s}_1 \otimes \boldsymbol{\kappa}_1\ \boldsymbol{s}_2 \otimes \boldsymbol{\kappa}_2\ \cdots\ \boldsymbol{s}_N \otimes \boldsymbol{\kappa}_N \,\right] \tag{3}$$

is a matrix with $(2^N L) \times N$ dimensions, where $\otimes$ is the Kronecker product.

Since the modulus of the entries of $\tilde{\boldsymbol{S}}\boldsymbol{c}_s$ is usually not constant, additional intermodulation terms need to be introduced. It can be proved that for multi-carrier constant envelope multiplexing, the general intermodulation term has the following form

$$\boldsymbol{s}_{\mathrm{IM}} = \sum_{i=1}^{N} \boldsymbol{K}_i \boldsymbol{c}_{K_i} + \tilde{\boldsymbol{V}}\boldsymbol{c}_{\tilde{V}} \tag{4}$$

where $\boldsymbol{K}_i = \boldsymbol{s}_i \otimes \boldsymbol{\kappa}_i^{\perp}$ for $i = 1, 2, \cdots, N$, $\boldsymbol{\kappa}_i^{\perp}$ is the $L \times (L-1)$ dimensional matrix formed by the basis vectors of the orthogonal complement of $\boldsymbol{\kappa}_i$, $\tilde{\boldsymbol{V}} = \boldsymbol{V} \otimes \boldsymbol{I}$, where $\boldsymbol{I}$ is a L-dimensional unit matrix, $\boldsymbol{V}$ is a $2^N \times (2^N - N - 1)$ dimensional matrix composed of all the ith-order intermodulation term $\boldsymbol{s}^{(i_1, i_2, \cdots, i_k)} = \boldsymbol{s}_{i_1} \circ \boldsymbol{s}_{i_2} \circ \cdots \circ \boldsymbol{s}_{i_k}$ for $i = 2, 3, \ldots, N$, where $\circ$ is element-wise product, $\boldsymbol{c}_{Ki}$ and $\boldsymbol{c}_{\tilde{V}}$ are the linear combination coefficients of $\boldsymbol{K}_i$ and $\tilde{\boldsymbol{V}}$, respectively.

It is not difficult to verify that $\boldsymbol{s}_{\mathrm{IM}}$ is orthogonal to each $\boldsymbol{s}_i$. However, this orthogonality constraint is only

valid when all signal components are phase aligned. It is important to note that there is no restriction on the correlation value when the relative delay is within the range of plus or minus one spreading chip. For the single-frequency bipolar case, it can be proved that with the ideal spread sequence assumption, the constancy of the correlation between the integrated signal and every signal component before and after constant envelope reconstruction can be ensured. Nevertheless, for multicarrier cases, the term $\boldsymbol{K}_i\boldsymbol{c}_{K_i}$ for $i = 1, 2, \cdots, N$ in (4) may make the correlation value be nonzero at some nonzero relative delay. Therefore, in order to eliminate the interference of the intermodulation term in the phase rotated Type-III ACE-BOC technique on the shape of the correlation function, the ACE-BOC signal expression is first transformed into the form of

$$\tilde{\boldsymbol{s}}_{\mathrm{ACE}} = \tilde{\boldsymbol{S}}\boldsymbol{c}_s + \sum_{i=1}^{N} \boldsymbol{K}_i\boldsymbol{c}_{K_i} + \tilde{\boldsymbol{V}}\boldsymbol{c}_{\tilde{V}} \tag{5}$$

by using the intermodulation construction technique (Yao et al., 2016). By using the CEMIC technique, the following optimization problem

$$\begin{aligned} &\arg\min_{\boldsymbol{c}_v} \left\|\boldsymbol{c}_{\tilde{V}}\right\|^2 \\ &s.t. \left|\tilde{s}_{\mathrm{ACE},1}\right| = \left|\tilde{s}_{\mathrm{ACE},2}\right| = \cdots = \left|\tilde{s}_{\mathrm{ACE},2^N L}\right| \end{aligned} \tag{6}$$

is solved under the constraint of forcing $\boldsymbol{c}_{K_i}$ to be zero, where $\tilde{s}_{\mathrm{ACE},i}$ is the ith entry of $\tilde{\boldsymbol{s}}_{\mathrm{ACE}}$. The detailed process in solving this optimization problem is given in Appendix B of Yao et al. (2017) as pseudo-code.

It can be seen from Fig. 7 that through CEMIC-based optimization processing, the residual intermodulation component is further suppressed, the influence of intermodulation interference is eliminated, and the ideal design state is reached. This can be seen more clearly from the evaluation results of the measured signal quality in Sect. "Signal quality assessment".

The optimized Type III ACE-BOC power ratio and multiplexing efficiency are shown in Table 5. The corresponding constellation diagram and PSD simulation under unlimited bandwidth are shown in Figs. 8 and 9, respectively. It can be seen that suppressing the influence of the intermodulation term is at the expense of the loss of a certain amount of actual signal power and multiplexing efficiency. Under unlimited bandwidth, the multiplexing efficiency is 71.22%, which falls back to the same efficiency of the Type III ACE-BOC multiplexing technique given in Table 3. Compared with the original Type III ACE-BOC multiplexing technique,

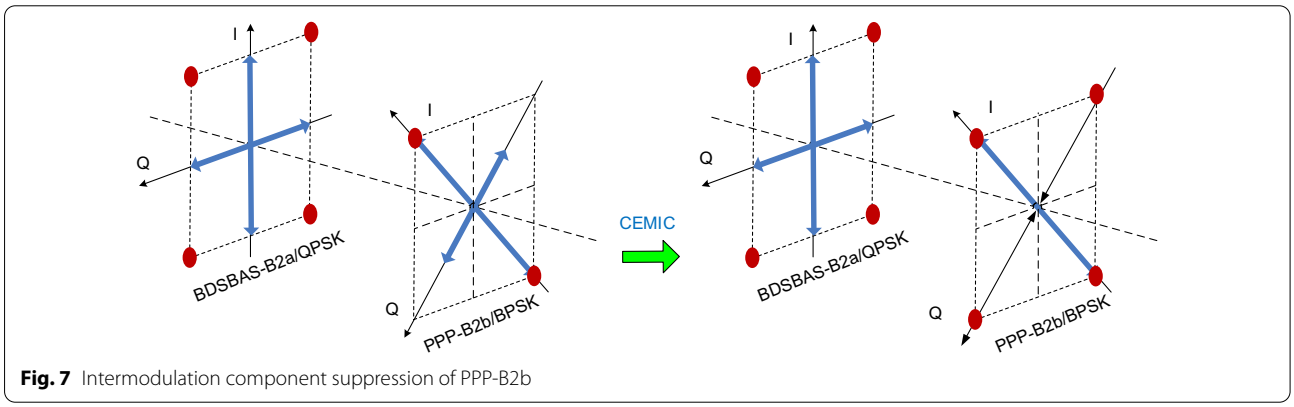

Fig. 7 Intermodulation component suppression of PPP-B2b

Table 5 Actual power and multiplexing efficiency of each component after phase rotation and intermodulation component suppression

B2a-I: B2a-Q: B2b-I: B2b-Q	Power proportion of different signals					Multiplexing efficiency	Phase relationship between B2b-I and B2a-I
	Bandwidth	B2a-I	B2a-Q	B2b-I	B2b-Q		
1:1:1:0	unlimited bandwidth	0.2374	0.2374	0.2374	0	71.22%	45°
	transmitting bandwidth	0.3118	0.3118	0.3118		93.54%	

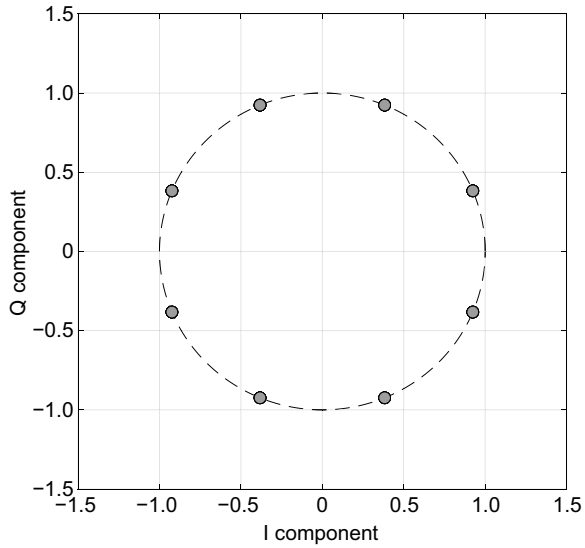

Fig. 8 Constellation of improved Type-III ACE-BOC multiplexing modulation

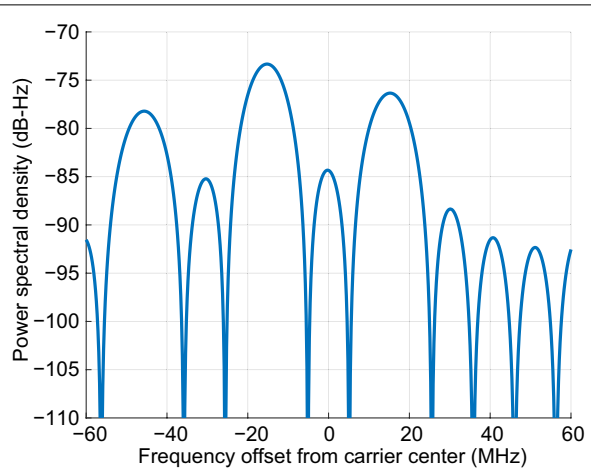

Fig. 9 Power spectral density of improved Type-III ACE-BOC multiplexing modulation

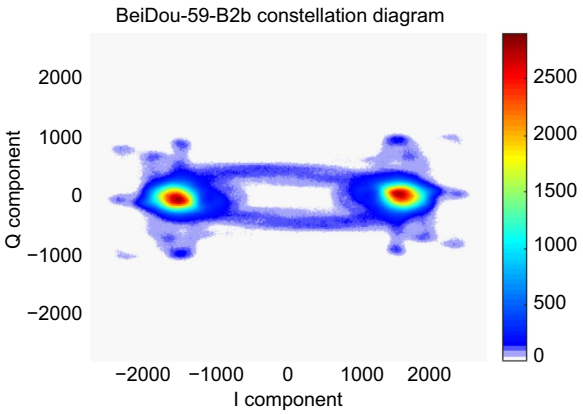

Fig. 10 Constellation when BDS-3 GEO-1 PPP-B2b is received separately

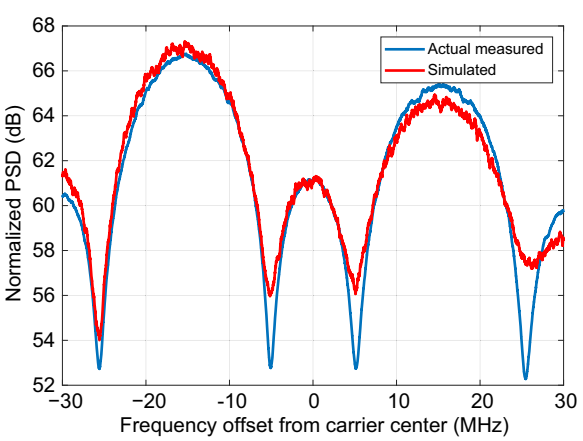

Fig. 11 Power spectrum of BDS-3 GEO-1 B2 signal

which was analyzed in Sect. "BPSK signal based on Type-III ACEBOC", the additional loss is 0.6 dB. However, it should be noted that the intermodulation term in the optimized ACE-BOC signal mainly exists at the higher harmonics of the subcarrier. Since the transmitting bandwidth of the actual transmitted B2 signal is 71.61 MHz, after the on-board filtering, the proportion of the intermodulation term in the actual transmitted signal is significantly reduced to only 6.46% of the total power. That is, the multiplexing efficiency under the transmitting bandwidth condition is 93.54%. Therefore, according to the current actual power state of the BDS-3 GEO satellite, there will be no significant impact on the service.

Signal quality assessment

In order to further verify the signal multiplexing performance, on June 23, 2021 the PPP-B2b signal broadcast from BDS GEO-1 satellite was continuously monitored and the data were collected using a 40-m antenna at the Haoping Observatory of the National Time Service Center of the Chinese Academy of Sciences. Signal quality evaluation software was used for analysis and processing.

Figure 10 shows the constellation diagram of the actual broadcast PPP-B2b signal in separately received mode. It can be seen that it is in the form of BPSK, and all the energy is concentrated on the I branch.

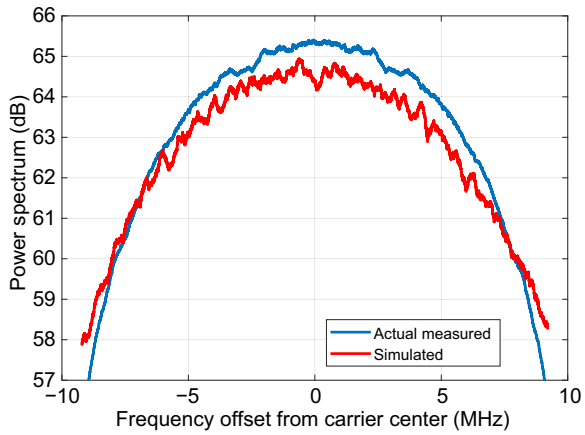

Fig. 12 Power spectrum of BDS-3 GEO-1 PPP-B2b

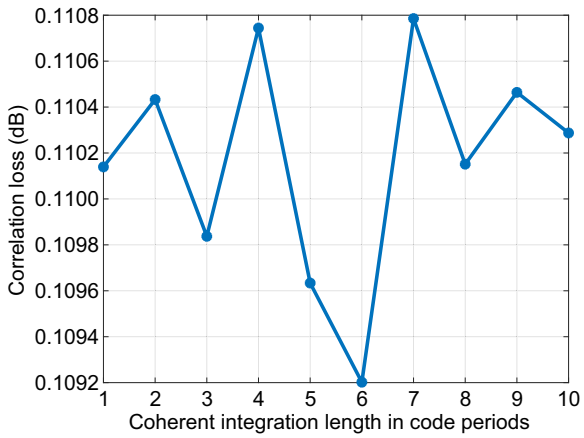

Fig. 14 Correlation loss when BDS-3 GEO-1 PPP-B2b_I is received separately

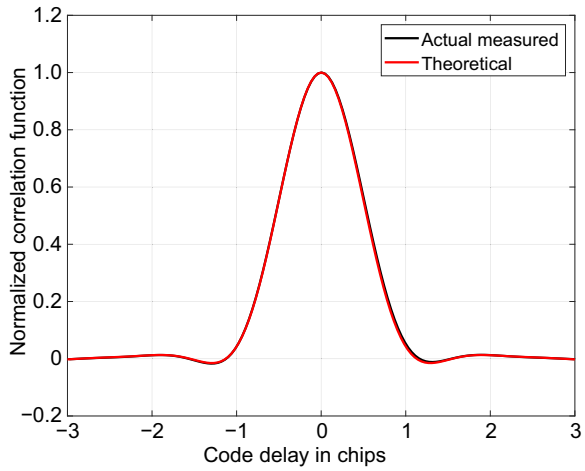

Fig. 13 Correlation function when BDS-3 GEO-1 PPP-B2b_I is received separately

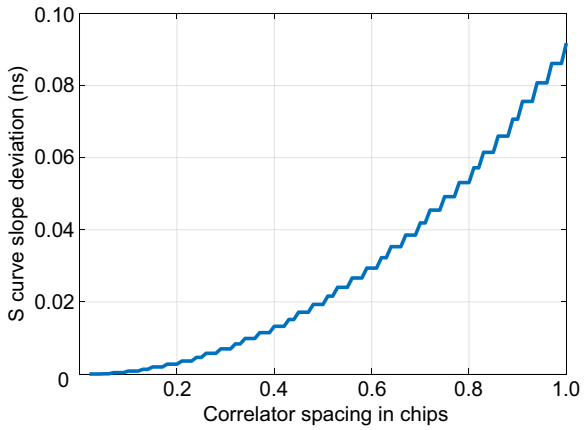

Fig. 15 S curve slope deviation of each signal component of PPP-B2b_I

Figures 11 and 12 show the power spectrum of the actual broadcast composite B2 signal and that of the PPP-B2b I component signal, respectively. It can be seen that under the reference bandwidth, the mean value of the measured power spectrum deviation is 0.228 dB, and the standard deviation is 0.571 dB, which is in good agreement with the simulated power spectrum curve and meets the design quality requirement of less than 1 dB.

Figures 13 and 14 show the correlation function and the correlation loss of the BDS-3 GEO-1 PPP-B2b I branch component in its separate receiving mode. It can be seen that the measured correlation loss under the reference bandwidth is 0.110 dB, which is in good agreement with the theoretical correlation function value, and the impact on the actual service is negligible. The results meet the performance requirements in the ICD that the correlation loss of PPP-B2b signal shall not exceed 0.6 dB.

Figure 15 shows the zero-crossing deviation of the code phase detection curve (i.e., S-curve) of the PPP-B2b I branch signal under the main lobe receiving bandwidth. Figure 16 shows the S-curve slope deviation of the PPP-B2b I branch signal with respect to the discriminator early-late spacing. It can be seen that the maximum deviation of the PPP-B2b I branch is 0.092 ns, and the S-curve slope deviation of the S curve is 1.558% on average, which meets the relevant design quality requirements of less than 0.5 ns and 10%.

Figures 17 and 18 show the actual broadcast PPP-B2b I branch baseband signal waveform and its digital distortion statistics. The statistics shows that the average length difference between the positive/negative chip and

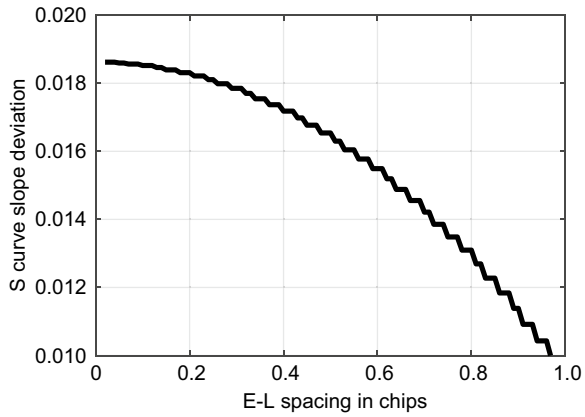

Fig. 16 S-curve slope deviation of BDS-3 GEO-1 PPP-B2b_I

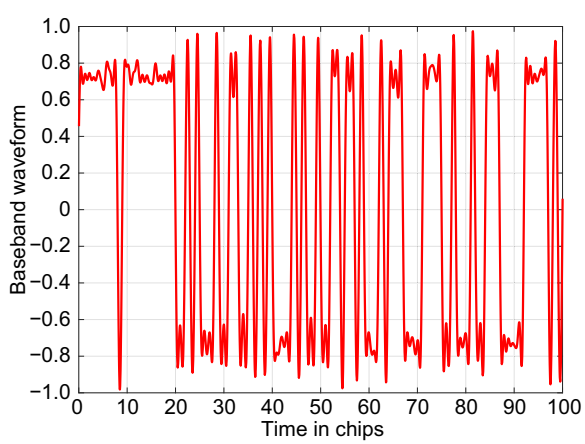

Fig. 17 Baseband waveform of BDS-3 GEO-1 PPP-B2b_I

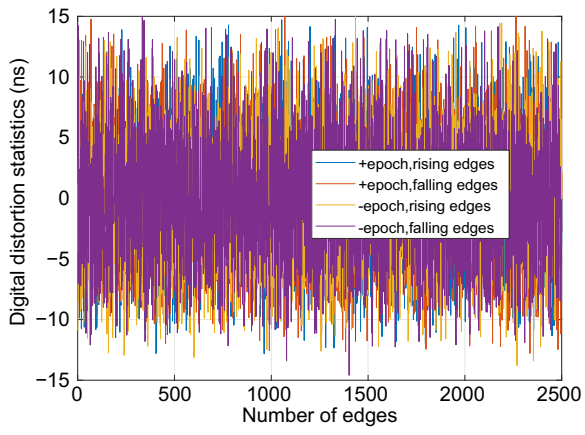

Fig. 18 Digital distortion statistics of BDS-3 GEO-1 PPP-B2b_I

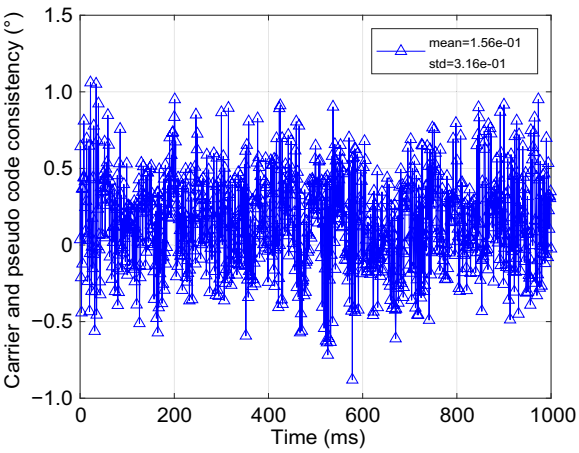

Fig. 19 Carrier and pseudo code consistency of BDS-3 GEO-1 PPP-B2b_I

the ideal chip is 0.0006 ns, and the standard deviation is 2.8409 ns, which meets the design quality requirements that the mean value should be less than 1 ns and the standard deviation should be less than 5 ns.

Figure 19 shows the carrier and pseudo code consistency of the broadcast PPP-B2b I branch. The statistics shows that the coherence between the carrier and the pseudo code is 0.082°, which is far less than the design quality requirements of 1° and shows a high degree of consistency.

Conclusions

The PPP service based on the B2b band of GEO satellites is one of the important services of BDS-3, and is an important measure for BeiDou to improve its high-precision service capabilities. However, the design of the PPP-B2b signal faces many constraints. On the one hand, because the B2a signal of GEO satellites is for safety-of-life in the civil aviation service, the addition of the PPP-B2b signal should not affect the B2a signal. On the other hand, the PPP-B2b signal should guarantee its own quality to ensure the reliable transmission of PPP corrections. Finally, it is also important to consider user compatibility for future upgrades.

Starting from the actual status and constraints of BDS-3 GEO satellites, this paper carries out research and design of the modulation and multiplexing techniques of the BDS PPP service signal based on ACE-BOC technique. From the aspects of transmission efficiency, multiplexing efficiency, and service forward compatibility, the PPP-B2b signal modulation technique based on Type III ACE-BOC multiplexing is proposed and optimized.

In view of the shortcomings caused by the intermodulation interference in the composite modulation, the phase rotation between the signal components reduces the proportion of the intermodulation components. On this basis, the CEMIC method is used for the optimization to further suppress the remaining intermodulation components that are not completely orthogonal to the useful signal components, and finally to construct a multiplexed composite signal based on the improved Type III ACE-BOC.

The constructed PPP-B2b signal was continuously monitored, and the data were collected using the 40-m antenna at Haoping Observatory. According to the evaluation, the averaged power spectrum deviation of PPP-B2b is only 0.228 dB, the correlation loss is 0.110 dB, the maximum deviation is 0.092 ns, the S-curve slope deviation is 1.558%, the averaged length difference between the positive/negative chip and the ideal chip is 0.0006 ns, and the coherence between the carrier and the pseudo code is 0.082°. The results show that the multiplexed composite signal generated by the improved Type III ACE-BOC proposed in this paper has good radio frequency characteristics, can achieve efficient information broadcasting and compatibility of BDS PPP services, and thus is an ideal solution that meets design constraints and requirements.

Acknowledgements
Not applicable.

Authors' contributions
Conceptualization and original draft preparation, C.L. and C.S.; Theory and methodology, Z.Y. and D.W.; Validation and data analysis, T.L. and Y.R.; data curation and supervision, D.L.; project administration, W.G. All authors have read and agreed to the published version of the manuscript. All authors read and approved the final manuscript.

Funding
This work was supported by China Association for Science and Technology (2019QNRC001); Young Innovation Foundation of Beijing National Research Center for Information Science and Technology (under Grant BNR2021RC01015); National Natural Science Foundation of China (Nos. 42074044 and 61771272).

Availability of data and materials
All data generated or analyzed during this study are included in this published article.

Declarations

Competing interests
The authors declare that they have no competing interests.

Author details
[1]Beijing Institute of Tracking and Telecommunication Technology, Beijing 100094, China. [2]Department of Electronic Engineering, Tsinghua University, Beijing 100084, China. [3]Space Star Technology, Beijing 100095, China. [4]Beijing Institute of Spacecraft System Engineering, Beijing 100094, China. [5]National Time Service Center, Academy of Sciences, Xi'an 710600, China.

Received: 21 October 2021 Accepted: 2 January 2022
Published online: 17 January 2022

References

Butman, S., & Timor, U. (1972). Interplex: an efficient multichannel PSK/PM telemetry system. *IEEE Trans. on Communication Technology*, COM-20(3).
Cabinet Office. (2018a). Quasi-Zenith satellite system interface specification centimeter level augmentation service (IS-QZSS-L6–001). November 2018.
Cabinet Office. (2018b). Quasi-Zenith satellite system performance standard (PS-QZSS-001). November 2018.
China Satellite Navigation Office. (2019a). The application service architecture of BeiDou navigation satellite system (Version 1.0). In.
China Satellite Navigation Office. (2019b). BeiDou navigation satellite system signal. Space Interface Control Document Open Service Signal B2b (Beta Version). December 2019, http://en.BeiDou.gov.cn.
China Satellite Navigation Office. (2019c). BeiDou navigation satellite system signal. Space Interface Control Document Open Service Signal PPP-B2b (Beta Version). December 2019, http://en.BeiDou.gov.cn.
China Satellite Navigation Office. (2019d). Development of the BeiDou navigation satellite system (Version 4.0). December 2019, http://en.BeiDou.gov.cn.
Dafesh, P., & Cahn, C. (2001). Phase-optimized constant-envelope transmission (POCET) modulation method for GNSS signals. Paper presented at the Proceedings of the 22nd International Technical Meeting of the Satellite Division of the Institute of Navigation (Ion Gnss 2009).
Dafesh, P., & Cahn, C. (2011). Application of POCET method to combine GNSS signals at different carrier frequencies. *Proc. ION ITM*, San Diego, CA, USA, 1201–1206.
Guo, S., Liu, C., Gao, W., & Lu, J. (2019). Construction and development of satellite navigation augmentation systems (in Chinese). *GNSS World of China, 44*(2), 1–12.
Guo, F., Yao, Z., & Lu, M. (2016). BS-ACEBOC: A generalized low-complexity dual-frequency constant-envelope multiplexing modulation for GNSS. *GPS Solutions, 21*(2), 561–575. https://doi.org/10.1007/s10291-016-0547-8
Hayes, D. (2018). *Galileo programme update*. ICG-13, Xi'an, China. December 2018.
Hayes, D., & Hahn, J. (2019). *2019-Galileo programme update*. ICG-14. Bangalore, December 2019.
Hein, G. W. (2020). Status, perspectives and trends of satellite navigation. *Satell Navig, 1*(22), 1–12.
Huang, Q., Song, L., & Wang, Z. (2017). Set message-passing decoding algorithms for regular non-binary LDPC codes. *IEEE Transactions on Communications, 65*(12), 5110–5122.
Huang, Q., Zhang, M., Wang, Z., & Zhang, X. (2019). FEC design for remote control and data transmission of aeronautic and astronautic vehicles. *Chinese Journal of Aeronautics, 32*(1), 159–166.
Huang, X., Zhu, X., Tang, X., & Ou, G. (2015). Asymmetric AltBOC modulation and its generalised form for BeiDou B2 signals. *Electronics Letters, 52*(2), 146–148.
Héroux, P., & Kouba, J. (2001). GPS precise point positioning using IGS orbit products. *Physics and CheMistry of the Earth, Part A: Solid Earth and Geodesy, 26*(6–8), 573–578. https://doi.org/10.1016/s1464-1895(01)00103-x
ICAO NSP DFMC SBAS SARPs Sub-group (DS2) (2018). *DFMC SBAS SARPs part A (v2.1)*. ICAO NSP 5th Meeting, Montreal, Canada. November 2018.
Jin, S., & Su, K. (2020). PPP models and performances from single- to quad-frequency BDS observations. *Satellite Navigation, 1*(16), 1–16.
Lestarquit, L., Artaud, G., & Issler, J.-L. (2008). AltBOC for Dummies or Everything You Always Wanted to Know About AltBOC. Paper presented at the *ION GNSS 2008*, Savannah, GA
Li, Z. (2017). Improving availability and accuracy of GPS/BDS positioning using QZSS for single receiver. *Acta Geod Geophys, 52*, 95–109.
Liu, C., Gao, W., Liu, T., Wang, D., Yao, Z., & Gao, Y. (2020). Design and implementation of a BDS precise point positioning service. *Navigation-Journal of the Institute of Navigation, 67*(4), 875–891.
QZSS. (2018). Centimeter level augmentation service (CLAS). Retrieved from https://qzss.go.jp/en/overview/services/sv06_clas.html.
Revnivykh, I. (2019). *GLONASS and SDCM status and development*. Paper presented at the ICG-14, Bengaluru, India. December 2019.

SBAS IWG. (2016a). *Satellite-based augmentation system dual-frequency multi-constellation definition document*. Paper presented at the 31th SBAS IWG, Dakar, Senegal. November 2016.
SBAS IWG. (2016b). *Satellite-based augmentation system dual-frequency multi-constellation interface control*. Paper presented at the 31th SBAS IWG, Dakar, Senegal. November 2016.
Spilker, J. J., & Orr, R. S. (1998). Code Multiplexing via Majority Logic for GPS Modernization. Paper presented at the ION GNSS 11th International Technical Meeting of the Satellite Division, Nashville, TN, US.
Yang, Y., Gao, W., Guo, S., Mao, Y., & Yang, Y. (2019). Introduction to BeiDou-3 navigation satellite system. *Navigation, 66*(1), 7–18.
Yao, Z., Guo, F., Ma, J., & Lu, M. (2017). Orthogonality-based generalized multi-carrier constant envelope multiplexing for DSSS signals. *IEEE Transactions on Aerospace and Electronic Systems, 53*(4), 1685–1698. https://doi.org/10.1109/TAES.2017.2671580
Yao, Z., & Lu, M. (2017). Signal multiplexing techniques for GNSSs. *IEEE Signal Processing Magazine, 34*(5), 16–26. https://doi.org/10.1109/msp.2017.2713882
Yao, Z., Zhang, J., & Lu, M. (2016). ACE-BOC: Dual-frequency constant envelope multiplexing for satellite navigation. *IEEE Transactions on Aerospace and Electronic Systems, 52*(1), 466–485. https://doi.org/10.1109/TAES.2015.140607
Zhang, K., Zhou, H., & Wang, F. (2013). Unbalanced AltBOC: A Compass B1 candidate with generalized MPOCET technique. *GPS Solutions, 17*(2), 153–164.

Publisher's Note